Eng. & Technology, Vol.25, No.7, 2007

Improving Oxidation Resistance of Stainless Steel (AISI 316L) by Pack Cementation

Dr. Ahmad Ali Moosa * Dr. Muna Khedeir Abbas* Mr. Rajab Mohammed*

Received on: 4/6/2007
Accepted on: 18/9/2007

Abstract

The cyclic oxidation resistance of austenitic stainless steel (AISI 316L) can be improved by enriching the surface composition in Al and Si using pack cementation process. In this work, stainless steel is coated with two different types of coatings, the first one is Si-modified aluminide coating and the second is the Ce-doped silicon modified aluminide coating. Aluminum, silicon with and without cerium were simultaneously deposited by diffusion into St.St.316L substrate by the pack-cementation process, using a pack mixture containing (18%A1, 7%Si, 2%NH_4C1 and 73%Al_2O_3) and 0.5% Ce (wt %) when required.

Microstructure and chemical composition of the coated specimens were analyzed using electron microscopy (SEM) with energy dispersive spectroscopy (EDS). X-Ray diffraction (XRD) was used to identify phase formed in the surface layer of as-coated specimens. The coating time was changed, and it was found that diffusion coating time of 3h at 970C° produces coating thickness of 160-180µm and consist mainly of FeAl and ($Cr_4Si_4Al_{13}$) phases. Also, the surface morphology for the coated samples after 3h coating time at 970C° are dense, smooth and homogeneous. Cyclic oxidation tests were conducted on the uncoated St.St.316L , Si-modified aluminide coating and on Ce-doped silicon modified aluminide coating at a temperature range between (700-900)C° in (air and H_2O) for 120h at 10 h cycle.

The oxidation kinetics for uncoated St.St.316L in air environment are found to be linear, while the oxidation kinetics at water vapor environment are found to be nearly parabolic. The linear rate constant (K_L) and the parabolic rate constant (Kp) values obtained at 800C° in air and water vapor are $-2.77*10^{-7}$(mg/cm^2)/s and $2.18*10^{-5}$(mg^2/cm^4)/s respectively. The phases present on the cyclic oxidation of uncoated St.St.316L surface under most test conditions as revealed by XRD analysis are chromium (III) oxide, $NiFe_2O_4$, $NiCr_2O_4$ and iron oxide. Oxide phases that were formed on coated systems during air and H_2O oxidation exposure condition are $FeAl_2O_4$, $Fe(Al,Cr)_2O_4$ and Fe_2O_3. The oxidation kinetics for both coated systems in air and water vapor are found to be linear and parabolic respectively.

تحسين مقاومة الأكسدة للفولاذ مقاوم الصدأ الأوستنايتي (AISI 316L) بطريقة الطلاء بالسمنتة

الخلاصة

تشير نتائج الدراسة الحالية الى امكانية زيادة مقاومة التأكسد للفولاذ مقاوم الصدأ الأستنايتي (AISI 316L) وذلك بزيادة محتوى الالمنيوم والسليكون عند سطح الفولاذ بأستخدام تقنية الطلاء بالسمنتة (Pack Cementation) .

في هذه الدراسة تم طلاء الفولاذ (٣١٦L) بنظامين من الطلاء (Coated Systems). النظام الاول فولاذ ٣١٦L / الالومنياید المدعم بالسليكون، إما النظام الثاني فولاذ ٣١٦L /الالومنياید المدعم بالسليكون والسيريوم. تم إجراء ترسيباً انياً بالألمنيوم والسليكون تارة وبالألمينوم والسليكون والسيريوم تارة اخرى على الفولاذ مقاوم الصدأ الاستينايتي (٣١٦L) بأعتماد ألية الطلاء الانتشاري، وبأستخدام خليط مكون من(73%Al_2O_3, 2%NH_4Cl, 7%Si, 18%Al) بالأضافة الى Ce ٠,٥% عندما يكون ذلك مطلوباً. تم تحليل التركيب المجهري والتركيب الكيميائي للعينات المطلية بأستخدام المجهر الالكتروني الماسح (Scanning Electron Microscopy) وملحقاته (Energy Dispersive spectroscopy)

* Production and Metallurgy Eng. Department, University of Technology, Baghdad- Iraq

http s://doi.org/10.30684/etj.25.7.9
2412-0758/University of Technology-Iraq, Baghdad, Iraq

لمعرفة تركيز عناصر الطلاء في سطح العينة المطلية ، كما تم تحديد الاطوار المكونة بعد الطلاء في سطح العينة المطلية بأستخدام جهاز حيود الأشعة السينية (X-Ray Diffraction) . تم تغيير زمن الطلاء وقد وجد بأن زمن الطلاء ٣ ساعات عند درجة حرارة ٩٧٠مْ هوالزمن المثالي لعملية الطلاء وكان سمك طبقة الطلاء يتراوح مابين (١٦٠-١٨٠) مايكرون . وأن سطح هذه الطبقة يتكون من الطور AlFe والطور $Cr_4Si_4Al_{13}$.أن طبيعة طبقة الطلاء عند هذا الزمن (٣ ساعة) وهذه الدرجة الحرارية (٩٧٠مْ) يتميز بأنه سطح ناعم ومتراص ومنتظم .

جرت أختبارات التأكسد بشكل دوري (Cyclic Oxidation Test) للفولاذ مقاوم الصدأ الأوستينايتي(٣١٦L)(بدون طلاء) ونظامي الطلاء : فولاذ ٣١٦L/ الالومينايد المدعم بالسليكون وفولاذ ٣١٦L/ الالومينايد المدعم بالسليكون والسيريوم في أوساط مختلفة هي: الهواء وبخار الماء عند درجات الحرارة (٧٠٠-٩٠٠) مْ. اختبارات الأكسدة هذه جرت لمدة ١٢٠ ساعة وبمعدل ١٠ ساعة للدورة الواحدة.

تشير نتائج الدراسة الحالية الى أن السلوك الكيناتيكي العام للتأكسد للفولاذ مقاوم الصدأ(٣١٦L) يتبع القانون الخطي في وسط الهواء بينما في وسط بخار الماء يتبع تقريباً قانون القطع المكافئ. وكانت قيم ثابت معدل التأكسد الخطي (K_L) وقيم ثابت معدل التأكسد (Kp) عند درجة حرارة ٨٠٠مْ في وسطي التأكسد الهواء وبخار الماء هي ($2.18*10^{-5}$ mg^2/cm^4)s , $-2.77*10^{-7}$(mg/cm2)s) على التعاقب .أظهرت نتائج التحليل بحيود الاشعة السينية ظهور أطوار أوكسيدية على سطح الفولاذ مقاوم الصدأ (٣١٦L)(بدون طلاء) في معظم أختبارات التأكسد . Chromium (III) Oxide, $NiFe_2O_4$, $NiCr_2O_4$, Fe_2O_3. تشير النتائج إلى إن السلوك الكيناتيكي لتأكسد نظامي الطلاء يتبع القانون الخطي وقانون القطع المكافئ في وسطي الهواء وبخار الماء على التعاقب .

1. Introduction:

The performance of different alloys exposed at high temperature depends upon their mechanical resistance as well as their corrosion / oxidation properties. When the mechanical requirements are not critical, austenitic stainless steels may play a role in substituting the more expensive Ni and Co base alloy [1]. Stainless steels are those alloys of iron and chromium, with or without other elements, containing at least 11% chromium [2, 3]. This is the minimum amount of chromium necessary to form a stable passive chromium oxide film. It is this film that is the basis for the corrosion resistance of all stainless , and most nickel base , corrosion - resistance alloys[3,4,5,6].

1.1 Codeposition of Steels:

The codeposition of two or more elements is a halide -activated cementation pack which is inherently difficult because of large differences in the thermodynamic stabilities for there volatile halides [7].

When a binary master alloy powder is used (e.g , Cr-Al ,Cr-Si, or Al-Si) both elements can be codeposited into the substrate simultaneously, if each element has significant and comparable partial pressures for the transporting gaseous species the designed surface composition for the coated substrate can be achieved by careful control of the master alloy composition (i.e, the thermodynamic activities of the metallic components) and the choice of an activator salt of suitable stability [8] .

The early stages of this codeposition technology have relied on the use of previously manufactured master alloy powders, which are relatively expensive. By the use of a master alloy in the pack, the thermodynamic activity of the normally favored element could be reduced, such that with the proper choice of halide activator salt and process temperature, codeposition e.g of Cr-Si, Al-Si, or Cr-Al into steels, become possible[9]. Miller et al [10] codeposited Cr-Al diffusion coating on low -alloy steel and stainless steels, respectively, using a 85Cr-15Al master alloy powder as a pack component. The surface composition sought by those studies was Fe-20Cr-4.5Al corresponding to the commercial Kanthal alloy. By that method, the surface compositions were very sensitive to the thermodynamic activity of Cr in the master alloy. As the thermodynamic activity of Al was held

intentionally very low, the Al content introduced at the surface was sometime not sufficient to push the carbon into the steel substrate. Thus for higher – carbon steels, by that process, a blocking external carbide film was formed at the surface and the substrate was decarburized. The external carbide disrupted the inward diffusion of Al and Cr, while decarburization reduced the strength of the steel. However, the simultaneous introduction of Si with Cr acts to push carbon into the substrate because of a strong thermodynamic repulsion between Si and C, and the surface layer is transformed from austenite to ferrite. Because ferrite has a very low solubility for carbon , the outer carbide layer can be avoided , and ferritic coating can support rapid growth [11].

In fact, the Cr-Si codeposition into steel has now been achieved by the use of pure powder of Cr and Si , instead of the earlier Cr-Si master alloy technology [12]. A single step codeposition process would be cheaper, easier, and better than a two-step process the resulting concentration, profiles would be more effective oxidation and hot corrosion resistant.

Recently, Rapp, Wang and Weisert [13] have developed procedures for the codeposition of Al and Cr simultaneously into iron -base alloys to achieve kanthal like surface compositions on pure Fe and Fe- 2.25Cr -1Mo substrates which produced protective Al2O3 scales upon oxidation. Also, the codeposition of Cr and Al on 304 stainless .steel has been investigated by N. H. Heo et al. [14]. A codeposited coating layer , which shows high oxidation resistance , is mainly characterized by three zones ; an outer layer of iron aluminide, a nickel - rich iron aluminide and an interdifflusion zone consisting of alpha (α) ferrite and nickel aluminide precipitates. Oxidation resistance increased as the thickness of the outer iron aluminide layer increased. This means that the Al in the outer layer, rather than that in nickel aluminide precipitates or alpha ferrite, acts as a strong aluminium source forming a protective Al_2O_3 scale at the coating surface.

1.2 Aim of This Work

The aim of this work is to develop a new technique to deposit Al, Si, and cerium simultaneously by pack cementation on the surface of austenitic stainless steel (316L), using a single step pack cementation process. This single step process is a new technique for deposition of three elements, which will reduce the use of materials, labor, time , energy and improve the coating life by adding cerium at the surface of a component. This will be called cerium-doped silicon modified aluminide diffusion coating.

2. Experimental Works

2.1 Materials:

The substrate alloy used in this study was austenitic stainless steel (316L). The nominal composition and the spectrochemical analysis are shown in Table (1).

The austenitic stainless steel (316L) samples were cut into disc shape 20 mm in diameter and 3mm thick . Small whole 2mm diameter was drilled in each sample for holding. All the surfaces, including the edges were wet ground 120, 220, 320, 500, 600, 800, 1000 and 1200 grit silicon carbide papers. These samples were then cleaned with water, degreased with acetone and than ultrasonically cleaned for 30 minutes. The dimensions of all samples were measured.

The weight of each sample was measured using a Mettler microbalance (Sartorrus, Germany), with an accuracy of ± 0.01 mg .The balance was calibrated frequently using standard weights. Prior to weighting, all samples were held over night in glass desiccators in order to eliminate any effect of humidity on the sample weight determination.

2.2 Pack Cementation

Many experimental works were

carried out to investigate the feasibility of simultaneous deposition of aluminum and silicon, and simultaneous deposition of aluminum, silicon and cerium on austenitic stainless steel (316L) by pack cementation process to increase its high temperature durability in oxidation and corrosive environment. A series of further experiments were performed to investigate the effects of pack compositions, deposition temperature and time coating on kinetics coating growth process. The following details of pack cementation process represent the optimum diffusion coating that could be obtained in this study.

2.3 Pack Powder

2.3.1 Silicon-Modified Aluminide Diffusion Coating Pack Mixture

The pack mixture used for silicon - modified aluminide diffusion coating, consist of 18wt.% Al powder (50-150μm in particle size) as an aluminum source (Riedel-de Haen AG-Germany), 7wt.%Si powder (70-150μm in particle size) as Si source (BDH chemicals Ltd. Poole England), 2wt% NH4Cl as activator (chem.-supply, Ltd; Australia) and the balance was α-alumina powder (70-210 μm in particle size) (BDH Chemicals Ltd Poole England) as the inert filler . The NH4Cl was dried in an oven at 90C° for 24hr before mixing with other powders. The pack powder was mixed in a ball mill (type 05.102-manufactured by Fritsch Pulaeristte-Germany) at 300 rpm for 180min. with the addition of n-hexane (n - C_6H_{14}) in order to prevent powders oxidation due to frictional heat (balls and liners made of porcelain material to prevent pack contamination). The pack was then dried at 75Cº for 10 hours according to Won et el. Procedure [15].

2.3.2 Cerium Doped Silicon - Modified Aluminide Diffusion Coating Pack Mixture

The pack mixture used is the same as in silicon - modified aluminide diffusion coating pack except 0.5wt% of the pack alumina filler was replaced with cerium as a reactive element oxide, assay 99.9% (Fluka, Switzerland).

2.4 Pack Cementation Process:

The stainless steel (316L) sample was placed in a stainless steel cylindrical retort of 50mm in a diameter and 80mm in a height in contact with the pack mixture. The retort was then put in another stainless steel cylindrical retort of 80mm in a diameter and 140mm in a height. The outer retort has a side tube through which argon gas pass and second hole in the top cover for argon gas out let. Type- k thermocouple was inserted through the cover of outer retort for recording real temperature near inner retort. Figure(1) shows the apparatus used for pack cementation. This combined system was then put in an electrical holding furnace under an argon atmosphere with a flow rate of 1.5L/min. Once the inert atmosphere had been established, heating cycle started for diffusion coating as shown in Figure(2). For silicon-modified aluminized and cerium doped silicon modified aluminide pack cementation processes, the pack composition and heating cycle are shown in Table(2).

The argon atmosphere was maintained during all the diffusion coating process as well as cooling. The samples were then removed from the pack and ultrasonically cleaned for 30 minutes in ethanol to remove any loosely entrapped pack material on the surface, and weighed in order to determine the Al, Si pickup. No further heat treatment was done to the specimens after coating. Cross-section of each sample was mounted in a cold - setting epoxy. Grinding was conducted with successively finer silicon carbide papers from 220 to 1200 grit. The samples were then polished using 5.0μm and 0.3μm alumina suspension sequentially. These samples were than cleaned and the microstructures of the coated layers were observed. Cross sections and coating morphology were examined using light optical microscope (LOM) type

(CARLZEISS JENA, DDR). For this purpose optical microscopy fitted by digital camera type (Smartic with 5 mega pixels resolution) was used.

Several experiments with different coating times were conducted to obtain the best coating thickness. It was found that diffusion coating time of 3 hours at 970Cº produces average coating thickness of 170µm.

2.5 Cyclic Oxidation:

Cyclic oxidation at high temperature and at different environments of air and water vapor (H_2O) were conducted in order to study the thermal shock and oxidation resistance of austenitic stainless steel (316L) with and without silicon-modified aluminide diffusion coating and with cerium doped silicon-modified aluminide diffusion coating.

During cyclic oxidation, the furnace temperature was controlled within ±3C° by using Ni-chrome thermocouple type K. The thermocouple was inserted into the furnace chamber through an access hole on the tope of the furnace and positioned in the proximity of the samples. The thermocouple was calibrated at three standard temperatures of boiling water, tin melting point, and aluminum melting point. The evaluation of the oxidation resistance of the coatings has been carried out by heating the samples in a furnace at test temperature and weighing them every 10 h. the samples were removed from the furnace, allowed to cool, ultrasonically cleaned in ethanol to detach the spalled oxide and the weight change per unit surface area was determined according to Martinengo et al procedure [16].

2.5.1 Oxidation in Dry Air

Austenitic stainless steels (316L) with and without silicon-modified aluminide diffusion coating , and with cerium doped silicon-modified aluminide diffusion coating samples were accurately weighed and then placed into ceramic crucibles . Cyclic oxidation tests were carried out in a Carbolite programmable furnace (manufactured by Sheffield, England) in the temperature range 700C°-900C° in air at 1 atmospheric pressure. Each heating cycle includes heating in the furnace for 10 hours at the test temperature and cooling in still air. Samples weights changes before and after each oxidation cycle were measured. Normally, at least 3 weight measurements were taken.

2.5.2 Oxidation in Water Vapor

The cyclic Oxidation tests were conducted in water vapor in the temperatures range (700C°-900C)± 5C° and the samples of St.St.316L with and without silicon-modified aluminide diffusion coating, and with cerium doped silicon-modified aluminide diffusion coating. The experimental set up is shown in Figure (3). The tube furnace has a water vapor inlet, which permits a preheated vapor at test temperature before it makes contact with the samples. The reaction chamber was first heated to 200C° in air. Water vapor generated in an evaporator was introduced thereafter. The chamber was pumped with water vapor, the chamber was heated up to the desired temperature. After each oxidation cycle was allowed to cool to room temperature for interrupted weight-measurements after each cycle of 10h up to 120h of cumulative exposure at the respective test temperature.

2. 6 X- Rav Diffraction Inspection

A Riga Ku X-ray generator with Cu Kα radiation at 40 kv and 20mA was used. The X-ray was generated by electric diffractometer, type Philips (Pw 1840), operating at scanning speed of 6º (2θ) per minute. The detector was moved through an angle of 2θ=10 to 90 degrees. The XRD analysis was carried out at S.C. of Geological Survey and Mining.

2.7 Scanning Electron Microscopy

A Camscan 3200w scanning electron microscopy (SEM), equipped with a link energy dispersive X-ray spectroscopy (EDX) system , was used to examine the metallographic coating samples collected during the cyclic

oxidation experiments. The SEM was used to study the morphology of the external scales formed on these coatings testing, and to examine the phase changes in the coatings and substrates over time.

3- Results and Discussion

The coatings developed from the present experimental works on austenitic stainless (316L) in the case of simultaneous aluminizing –siliconizing coatings, shows that the coating times 3h, the best conditions obtained for coatings at temperature 970Cº.

Figure (4) shows the typical morphology by SEM of aluminized- siliconized of austenitic stainless steel (316L) coated in a pack composed of 18%Al, 7%Si and 2% NH_4Cl at 970Cº for 3h . According to the EDX analysis, this surface is composed of about 42.87wt% Al, 1.91 wt% Si . This composition suggests the formation of FeAl. XRD confirmed that the outer layer is the FeAl and $(Cr_4Si_4Al_{13})$84F. The results of X-Ray diffraction (XRD) in Fig. (A1) in appendix A analysis related that the surface of coating consisted mainly of FeAl, $(Cr_4Si_4Al_{13})$84F, and very small amount of Fe_5Si_3 phases was detected. The concentration of Ce in the coating was too low to be examined by EDX.

3.1 Cyclic Oxidation:

This section will examine the cyclic oxidation resistance of the uncoated austenitic stainless steel 316L and coated systems (silicon-modified aluminide and cerium-doped silicon modified aluminide diffusion coatings). The uncoated austenitic stainless steel (316L) was tested, to provide standard to be compared with the cyclic oxidation resistance of silicon modified aluminide coating, and the cerium-doped silicon modified aluminide coating. The role of cerium in improving cyclic oxidation resistance will be explained by linking literatures on the oxidation mechanisms of alloys containing reactive elements to the data collected in this study.

Cyclic oxidation evaluates oxidation resistance and thermal shock resistance. Thermal shock is very important as the loss of protective oxide scales from the base material will result in the premature failure of the engine component and due to oxide growth stresses [17].

In cyclic oxidation, the weight measurements are taken at various exposure times during cyclic oxidation testing, which represent the overall weight gain loss due to both oxide scale growth and oxide scale spallation. However, growth kinetics and morphologies of scales in aggressive environments (dry air and water vapour) and other features of scales will be illustrated and discussed. The results are given in terms of:

1- Specific weight change, presented in kinetics carves

2- Metallographic investigations.

3.1.1 Oxidation in Air

Studies of oxidation kinetics provide valuable information about the oxidation mechanism and the rate-limiting step of the total reaction oxidation rate measurements also commonly serve as basis for a quantitative numerical description of the oxidation behaviour.

Weights changing were recorded for kinetics identification in dry air in the temperatures range (700-900)Cº for up to l20h at 10h cycle the specific weight change data of the uncoated stainless steel 316L for each temperature tests is plotted in Figure (5) as a function of time . The initial kinetic is rapid, but the rate of weight change gradually decreases at longer times. The kinetics can be described by examining the growth rate time constant or n value, which is found as the exponent in the following rate equation [18]

$$\Delta W/A = kt^n \quad \ldots\ldots\ldots (1)$$

where ΔW is the weight change, A is the sample surface area, k is the rate constant, n is the growth- rate time constant, and t is the time of oxidation . From Figure (5), n-value for each

temperature is calculated from a computer program according to the best fit to Equation (1). At 800Cº, the n-values is 1.e, parabolic behaviors found. Another n values are shown in Tab1e (3). It is found that the relationship is parabolic when n=0.5 the exponential constant n characterizes the oxidation rate as follows: if n=1, the oxidation rate is liner, n=0.5 the oxidation is theoretically parabolic, if n=0.33, then the oxidation rate is cubic [19].

Deviation from theoretical value of n=0.5 can be explained by an oxide layer cracking to a sudden increase of the surface area in contact with oxygen and then accelerating the oxidation kinetics. The weight gain during the transient stage corresponds to the complete consumption of the chromium in the uncoated austenitic stainless steel 316L can be calculated. Indeed, lf most of the Cr content in the un coated austenitic stainless steel 316L is transformed into Cr_2O_3 and the weight gain of the NiO phase is neglected. These results show that the parabolic kinetics at this temperature range can be quantified on the modified parabolic rate law with the assumption that oxidation is controlled by diffusion mechanism and the grain boundaries are the only effective short circuit diffusion paths. The grain boundary diffusion mechanism provides an initially high oxidation rate. As time passes, oxide grain growth occurs, which decreases the number of easy diffusion paths and slows the oxidation rate. Therefore, the easy path ways cut off, and the oxidation rate is decreased beyond that for parabolic kinetics [20, 21].

For the parabolic kinetics, the rate equation takes the form:

$$\Delta W / A = k\, t^{0.5} \quad \ldots\ldots\ldots (2)$$

where k now refers to the parabolic rate constant. A plot of specific weight change vs. square root of time gives a line as in Figure(6), the slop is the parabolic rate constant in units of (mg / $Cm^2)/h^{1/2}$). The kp value is then squared to give kp in units of (mg^2/ Cm^4)/h), as in the following expression :

$$(\Delta W/A)^2 = Kpt \quad \ldots\ldots\ldots (3)$$

Figure(6) exhibits obvious scattering in the obtained data, this is attributed to the cyclic oxidation behavior. The linear oxidation rate constants for three series of experiments are calculated and the linear lines represent the least squares carve fits to the data in Figure (6), the linear oxidation rate constants (k_L) for the set of experiments are listed in **Table (3).**

Over the temperatures range from (700 to 900)Cº , the linear oxidation rate coefficients and thus the oxidation rates of austenitic stainless steel 316L in air , vary in magnitude from a low value of $2.77*10^{-8}$(mg/cm^2)/s at 700Cº to high value of -$6.48*10^{-5}$ (mg/cm^2)/s at 900Cº . The point to be noted is that the weight gain calculated by application of the linear oxidation rate coefficient in **Table (3)** with Equation (3) results in the weight of oxygen gained by the sample under cyclic oxidation . The point to be noted also is that the other values of n and k_L in this study are calculated with the same procedure explained above. Effect of oxidation behaviors as well as the microstructural stability of high temperature oxidation and protective coating is determined by combining the results of kinetics studies with extensive analytical investigations using light optical microscopy (L.O.M), and x-ray diffraction (XRD) analysis.

The results of uncoated austenitic stainless steel 316L cyclic oxidized in air at temperature between 700Cº and 900Cº for 120 h at l0h cycle (Figure 5 and Table 3), show that, the oxidation rates are increased as temperature increased. The results are in agreement with those given by Authors [1, 22].

Figures (7a and 7b) shows the oxidized surface features of uncoated stainless steel 316L being examined by

L.O.M at 900Cº for 120h at 10h cycle. The scale appears with numerous nodules and with scale spalling and cracking especially at 900Cº. A large number of voids exist at the scale/alloy interface and in the alloy are observed during the cyclic oxidation of uncoated stainless steel 316L as shown in **Figure (7)** .It is believed that these voids reduce the scale / alloy contact and hence facilitate spallation. These voids may act as concentration sites of thermal stresses induced during heating and cooling leading to crack formation in and spalling of the surface scale.

The phases of scale formed on uncoated austenitic stainless steel 316L in air after 120h at l0h cycle at temperatures range (700-900)Cº were examined by x-ray diffraction analysis (XRD). Fig. (A.2) in Appendix A illustrates the major phases expected on uncoated stainless steel 316L surfaces at oxidizing temperatures (700-900)Cº in air for 120h at l0h cycle the major phases that exist on uncoated stainless steel 316L alloy surfaces after cyclic oxidation in air at (700-900)Cº for 120h at l0h cycle are (Cr_2O_3)γ , chromium (111) oxide (Cubic) and spinel phases such as $NiCr_2O_4$ and $NiFe_2O_4$.

3.1.2 Oxidation in Water Vapor (H_2O)

The results of cyclic oxidation experiments conducted at 700-900Cº under water vapor condition of uncoated austenitic stainless steel 316L alloy for 120h at l0h cycle are presented in Fig. (8) in terms of specific weight change as a function of time. It is observed that weight gain increases as the temperature is increased. Uncoated austenitic stainless steel 316L alloy exhibits obvious fluctuated weight change during the test. Such weight changes indicated scale spallation effects were occurring during the test. The amount of scale damage as evaluated by cyclic oxidation test correlates with the long – term cyclic oxidation behavior. Values of n and kp are shown in Table (3).

The weight gain observed for the uncoated austenitic stainless steel 316L cyclic oxidized in water vapor condition at temperature between (700-900)Cº for 120h at l0h cycle is lower than that obtained the oxidation in air. Also the value of kp ($0.755*10^{-5}(mg^2/cm^4/s)$) for oxidation in H_2O at 700C° is three orders of magnitude higher than k_L value ($2.77*10^{-8}(mg/cm^2/s)$) obtained during oxidation in air at the same conditions. This result is in agreement with those given by authors [23,24]. In presence of water vapor, after an incubation period, the scale becomes non-protective as a result of change of the oxidation limiting process. The water vapor effect is especially apparent in the temperature range of (600-700)Cº , whereas at higher temperature hardly any effect was found .The destruction of the protective scale by water vapor does not only depend on the H_2O content but also on the H_2O /O_2 - ratio . At higher contents of H_2O and low contents of O_2 the oxidation initially also starts with a parabolic law, however with a slightly higher rate than in dry gas.

XRD results for uncoated stainless steel 316L oxidation in H_2O vapor in the temperature range (700-900)Cº are illustrated in Figure (A.3) in appendix A. Oxide phases formed on uncoated 316L alloy surface during oxidation exposure conditions to H_2O atmosphere are chromium (III) oxide (cubic), Cr_2O_3, Fe_2O_3, Fe_3O_4 and spinel phases $NiFe_2O_3$. This result is consistent with those given by Nebuo Otsuka et al. [25] were oxidized several Fe-Cr-Ni austenitic stainless steel [13-25wt% Cr , 15wt% Ni] in steam for 1000 h at (500-900)Cº.

The surface oxides formed were developed progressively with increasing temperature as shown in Fig. (9), which illustrates that, the contribution of the oxides formed at triple point of grain boundaries is found and increases with increased temperature. The mechanism of the growth of these scales was explained by dissociation of FeO.

Namely reaction of water to form Fe_2O_3 at the external surface yields hydrogen. Part of which is assumed to diffuse inward to form water vapor within voids by reaction and decomposition of FeO following this equation:

$FeO + H_2 = Fe + H_2O$ ---------- (4)

The generated water vapor in the voids of inner scale acts as a carrier gas for oxygen leading to oxide formation at the scale / alloy interface and internal oxides and hydrogen which back diffuses to react further with oxide at outer voids surface [26] .

In water vapor environment, Ni oxidation process is slower than that in oxygen environment and the rate of oxidation changes from parabolic to linear. This is believed to be a result of the difficulty in forming adsorbed oxygen atoms on the surface of NiO, which is considered a basic oxide surface, so that the adsorbed species are mainly hydroxyl irons OH^- that could not enter the scale of p-type oxide [27].

Chromium oxidizes faster in rapid growth, in water vapor. It seems that the catastrophic oxidation in the presence of water vapor of chromia forming alloys in induced by oxygen and hydrogen penetration within the protective scale and reaction at the alloy / scale interface forms a large amount of (nickel or iron) chromium spinel [28].

3.2 Oxidation of Coated Systems:

3.2.1 Oxidation in Air

Both silicon-modified aluminide and cerium-doped silicon modified aluminide coated austenitic stainless steel 316L substrates were subjected to cyclic oxidation. A primary aim was to study the kinetic of oxidation behavior of the coated system as a function of the environments. The weight change of the samples with both types of coated systems during oxidation is plotted as a function of time as shown in Figs. (10) and (11) respectively. The kinetic behavior of cyclic oxidation of the coated systems in air, (Si-modifled aluminide and Ce-doped silicon modified aluminide diffusion coating) at temperature between 700C°-900C° follows the parabolic rate as shown in Figs. (10) and (11) respectively. In coated systems case, oxidation rate coefficients are obtained and listed in Table (4).

Table (4) shows the Kp values obtained at 700C° for both coated systems which are about one order of magnitude lower than that for the uncoated austenitic stainless steel 316L under the same test conditions.

When coated systems containing Cr and Al are exposed to a high-temperature oxidation environment, $Al_2O_3$and Cr_2O_3 scales are formed on the surface of the alloy. These scales prevent the rapid oxidation of nickel and iron in the alloy, thereby eliminating the dissolution and inward may undergo a catastrophic oxidation [1]. Rameshwar et al. [29] confirmed that, at higher temperature the oxidation resistance was frequently lost due to oxide-scale failure and formation of iron oxides. Figs. (10 and 11) show the improvement in oxidation resistance of the Si- diffusion of oxygen .

By kinetic measurement and morphological examination, it appears that the addition of cerium to the silicon-modified aluminide coated St.St.316L substrate improved by the scale adherence and integrity. There are several mechanisms proposed to account for the beneficial effects of a reactive element addition (such as Ce). The predominant mechanism is that the development of enhanced bonding forces between the scale and substrate metal through preferential segregation of the reactive element to this interface [30].

The phase constitution of the coatings was determined using XRD analysis. The major phases in the as - called coated systems (cerium doped and undoped-silicon modified aluminide was found to be FeAl and (Cr_4 Si_4 Al_{13}) 48F) phases. Cyclic oxidation at oxidized test temperature between (700-900)C° resulted in the formation $FeAl_2O_4$,

$Fe(Al,Cr)_2O_4$, $FeAlO_3$, Fe_2O_3 and Ce_2O_3 on the sample surface and an anticipated, its amount increased with exposure duration. This is evident from Figs. (B.l and C.l) in appendix B and C, which show the X-Ray diffractograms of the coated systems corresponding to various cyclic oxidation test temperatures. In addition, no excessive scale spalling is noticed during the entire oxidation period. It is, however, interesting to note from these figures that the bulk coating phase FeAl dose not transform to lower aluminum-containing phase, such as Fe_3Al, even after 120hr of exposure. This is a clear indication of lower rate of aluminum loss from the coating due to the lack of spalling of the protective alumina layer. Thus, the coated systems in this study appear to be adequate in providing cyclic-oxidation protections to the St.St.316L to 900C°.

The morphology of scale on Fig. (12 a) consisted of a bulkily layer of Fe_2O_3 with is lands of Fe_2O_4, and an inner layer of $FeAl_2O_4$ at the scale-metal interface. The disappearance of Fe_2O_4 after 120h of oxidation probably occurred by the following reaction: Fig. (12 b) show cross section images of LOM of silicon-modified aluminide diffusion coated St.St. 316L substrates after cyclic oxidation in air at 800 C° and 900C° respectively, under the same oxidation conditions indicated before. FeO was not detected in the scale, nor does it exist in equilibrium with $A1_2O_3$, after 120h only Fe_2O_3, Al_2O_3, $FeA1O_3$, $Fe(Al,Cr)_2O_4$ and $NiAl_2O_4$ were detected.

The formation of Al_2O_3 or $FeA1_2O_4$ as a continuous layer leads to a reduction in the rate of oxidation by blocking the outward diffusion of Fe^{+2} cations. This results in further reaction of the Fe_2O_4 layer with oxygen or Al_2O_3 and eventually the external scale component becomes Fe_2O_3. Fig. (13) show cross section images of LOM of cerium-doped silicon-modified aluminide diffusion coated 316L alloy substrates after cyclic oxidation in air at 800C°, and 900C° respectively under the same oxidation conditions indicated before.

S. Seal et al. [31] show that, the reduction in the rate of oxidation is due to the segregation of Ce^{+3} and Ce^{+4} ions at the oxide grain boundaries, causing hindrance to cation migration. This can be due to fine-grained oxide layer formation that has taken place due to heterogeneous nucleation caused by the presence of a reactive oxide particle.

3.2.2 Oxidation in Water Vapor

A plot of the weight change Vs. time for cyclic oxidation test at temperatures between (700-900)C°, under water vapor condition for 120h at l0h cycle for austenitic stainless steel 316L with silicon modified aluminide and with cerium-doped silicon modified aluminide are shown in Figures(14 and 15). In both coated system case, the oxidation rate coefficients are illustrated in Table(5).

From Table (5) show that the Kp values obtained at (800-900)C° for both coated systems were lower than that for the uncoated 316L under the same conditions (Table 3).

It was observed that reaction rates under water vapor cyclic oxidation are induced because of hydrogen to permeate from water vapor environment. The rates of hydrogen permeation decrease with increasing chromium contents. This result is in agreement with those given by [32].

Figs. (B.2 and C2 *)* in appendix B and C represent XRD analysis of cerium undoped and doped-silicon modified aluminide coated austenitic stainless steel 316L substrates respectively, after cyclic oxidation under H_2O atmosphere at temperatures between (700-900) C° for 120h at l0h cycle. The major oxides appear is these diffractograms a Al_2O_3 and $FeAl_2O_4$. This result is in good agreement with those given by Susan et al. [33], it has been suggested that the spinel phase ($NiAl_2O_4$) conform by solid-state diffusion between NiO and $A1_2O_3$ at higher temperature. However, at

700C°, the diffusion rates are too low between the two oxides and, if present, the layer is too thin to be identified by XRD.

The improve oxidation resistance of cerium-doped silicon modified aluminide diffusion coating also attributed to enhancement scale plasticity due to the effect of cerium or cerium oxides (Ce_2O_3) which allows the scale to deform and thus accommodate stresses. In this study of the endurance of coated Stainless steel 316L in water vapor, the coated integrity, even under cyclic oxidation conditions, is important because water vapor can directly penetrate through any existing defects, such as cracks, to the bore alloy. However, the two coated systems studied do not show severe scale spalling and appeared uniform and smooth after thermal cycling as shown in Fig. (16).

4- Conclusions

1. With the coating times of 3h , the best conditions obtained are for the coating at coating temperature 970Cº.
2. Uncoated stainless steel (316L) exhibited linear oxidation rate dependence in air over the temperatures between (700-900)Cº, the oxidation rate constants varies from a($K_p=2.77*10^{-8}(mg/cm^2/s)$ at 700Cº to value of ($K_L= -6.48*10^{-5}$ $(mg/cm^2/s)$ at 900Cº.
3. Uncoated stainless steel 316L exhibited parabolic oxidation rate dependence in H_2O atmosphere over the temperatures between (700-900) Cº , the parabolic rate constant (K_p) varies from a ($K_p=0.755*10^{-5}(mg^2/cm^4/s)$ at 700Cº to a value of $K_p=2.69*10^{-5}(mg^2/cm^4/s)$ at 900Cº.
4. Both coated systems (Si-modified aluminide and Ce-doped silicon modified aluminide) revealed good cyclic oxidation resistance compared with uncoated stainless steel 316L as the same identified conditions and oxidation kinetics was following the parabolic and linear oxidation rates.
5. The addition of 0.5wt% Ce to Si-modified aluminide diffusion coated stainless steel 316L substrate reduces the scale spallation and oxide damage .
6. At (700-900) Cº, the water vapor effects may be very small to identify and the only effect at this temperatures range is in the selective oxidation.
7. Alumina oxide scale is not the only phase present on the surface of both coated systems, other phases are obtained such as $FeAl_2O_3$, $Fe(Al,Cr)_2O_4$, $FeAlO_3$ and iron oxides.
8. It appears that the presence of the FeAl coating provides good cyclic oxidation resistance.

References:

1. F.J. Perez, F. Pedraza, M.P. Hierro, J. Balmain and G. Bannet, “Growth of Oxide Scales upon Isothermal Oxidation of CVD-FBR Aluminide Coated Stainless Steel”, Surface and Coatings Technology, Vol. 153, issue l, 2002, pp. 49-58.
2. William D.Callister, Jr. “Materials Science and Engineering an Introduction” Sixth Edition, Joho Wiley &Sons, lnc. 2003.
3. Henry R. Clauser, “Industrial Engineering Materials”, McGRAW. Hill & KOGAKUSHA, LTD, 1975.
4. “Hand Book of Material Selection” Edited by Myer Kutz, Myer Kutz Associates, inc Copyright by John Wiley &Sons, New York, 2002.
5. A.K.Gupta & R.C Gupta,” Material Science” , Second Edition, S.chand & Company LTD, RAM Na GAR, New Delhi-110055, 1983.
6. David k. Febeck & Anthony G. Atkins,” Strength and Fracture of Engineering Solids”, Second Edition, Prentice-Hall, 1996.
7. Robert Bianco, Mark A. HarPer and Robert A. Rapp, ”Codepositing Elements by Halide-Activated Pack Cementation”, The Journal of the Minerals, Metals and Materials

Society (JOM), Vol.43, No.11, 1991 ,pp.20-25.
8. Robert A. Rapp, "Pack Cementation Diffusion Coatings for Iron-Base Alloys", Fossil Energy Advanced Research and Technology Development Materials program, DOE/FA AA1510100, Work Break Down Structure Element OSU-2, February 9, 1995, pp.1-12.
9. Si-Cheng Kung and Robert A-Rapp," Analysis of the Gaseous Species in Halide-Activated Cementation Coating Packs", Oxidation of Metals, Vol. 32, Nos. ½, 1989, pp.89-109.
10. D.M Miller, S.C. Kunng, S.D-Scarberry and R.A.Rapp, "Simultaneous Chromizing-Aluminizing Coating of Austenitic Stainless Steels", Oxidation of Metals, Vol.29, Nos. ¾, 1988. pp. 239-254.
11. Mark A. Harper and Robert A. Rapp, "Codeposited Chromium and Silicon Diffusion Coatings for Fe-Base Alloys Via Pack Cementation", Oxidation of Metals, Vol. 42, Nos. ¾, 1994, pp. 303-333.
12. M. Van Roode and L-Hsu,"Evaluation of the Hot Corrosion Protection of Coatings for Turbine Hot Section Components", Surface and Coatings Technology, 37, 1989, pp.461-481.
13. R.A. Rapp, D. Wang and T. Weisert, "In Metallurgical Coatings", M. Khobaib and R. Krutenat, eds (AMS. AlME, Warrendale, 1987), pp.131. in: Si-Cheng Kung and Robert A.Rapp," Analyses of the Gaseous Species in Halide-Activated Cementation Coating Packs", Oxidation of Metals, Vol.32, No.1/2, 1989, pp.89-109.
14. N.H. Heo, M.T .Kim, J.H. Shin, C.Y .Kim,"Simultaneous Chromizing and Aluminizing using Chromium Oxide and Aluminum :(11) on Austenitic stainless Steel", Surface and Coatings Technology, 124, 2000, pp.39-43.
15. C.W. Won, H.R. Lee, S.S. Cho and B.S. Chun,Effect of Boron on The Densification of Al-Ni Intermetallic Compounds by HPCS", Chungnam National University, Daejeona, Korea, 1997, pp.415-419.
16. P.C. Martinengo and C. Carughi, U. Ducati and G.L. Coccia, "High Temperature Behavior of Protective Coatings on Ni-Base Superalloys, In: Materials and Coatings to Resist High Temperature Corrosion", Applied Science Pub.LTD, London, 1978, pp293-312.
17. Timothy James Rayner, "Development and Evaluation of Yttrium Modified Aluminide Diffusion Coatings", MSc, Thesis, University Toronto, Canada, 1998.
18. Parm. Valentin Rohr "Development De Reventements Pourles Aciers D' Exchangers Thermiques ET Amelioration Delewr Resistance Ala Corrosion En Environment Simulant Les Fumees De Combustion De Charbon", These, Institute National Polytechnique De, Toulouse, 2005.
19. S. Hayashi and T. Narita, "Competitive Effect of Water Vapor and Oxygen on the Oxidation of Fe-5 wt % Al Alloy at 1073k", Oxidation of Metals, Vol.56, No.3/4, 2001, pp.251-269.
20. V. Raghavan, "Materials Science and Engineering", a First Copy, (3d Edition), Prentice-Hall of India, Private Limited, new Delhi 110001,1989, pp.296-310.
21. B. Bieraggi, "Comments on Growth Rates of Alumina Scales on Fe-Cr-Al Alloys", Oxidation of Metals, Vol.64, Nos.516, 2005, pp. 397-403.
22. P. Kofstod, A. Rahmel, R.A. Rapp and D.L. Douglass, "International Workshop on New Fundamentals of Scale Growth", Oxidation of Metals, Vol.32, No.1/2, 1989, pp.125-166.

23. Khalil Al-Hatab, "Effect of Environments on Oxidation Behavior of Inconel Alloy 600", Ph.D Thesis , University of Technology, Department of Production Engineering and Metallurgy, Iraq, 2004.
24. E. Otero, A. Pardo, M.C .Merino, M.V. Vtrilla, M.D. Lopez and J.L. Delpeso, "Corrosion Behavior of IN-800 Superalloy in Waste-Incineration Environments: Hot Corrosion By Molten Chlorides", Oxidation of Metals, Vol.51, Nos.5/6, 1999, pp.507-520.
25. Nebuo Qtsuka, Yoshiaki Shida and Hisao Fujikawa, "Internal-External Transition for Oxidation of Fe-Cr-Ni Austenitic Stainless Steel in Steam", Oxidation of Metals,Vol.32, Nos.1/2, 1989 ,pp.13-45
26. G.H. Meier and F.S Pettit,"High-temperature Corrosion of Alumina-Forming Coatings for Superalloy", Surface and Coatings Technology, 39/40,1989,pp.1-17.
27. A. Galerie and L .Antoni, "Abnormal Oxidation of Stabilized Ferritic Steels in Water Vapor," Material Science Forum, Vol. 369-372, 2001. In: K.Al-Hatab," Effect of Environments on Oxidation Behavior of Inconel Alloy 600, Ph.D Thesis, University of Technology ,Baghdad, Iraq, 2004 .
28. P. Berthod, "Kinetics of High Temperature Oxidation and Chromia Volatilization for a Binary Ni-Cr Alloy", Oxidation of Metals, Vol.64, NOs.3/4, 2005, pp.235-252.
29. Rameshwar Jha, Colin W. Hawarth and Bemard B. Argent, "The Formation of Diffusion Coatings on some Low- Alloy Steels and their High temperature Oxidation Behavior: Part 2. Oxidation Studies", Calghad, Vol.25, Issue 4, 2001, pp.667-689.
30. A.A. Moosa, "Mechanism of Oxide Adherence on Ni-0.1 wt% Ce", Eng. Technology, Vol.20, 2001, pp.19-29.
31. S. Seal, S.K. Roy, S.K. Bose and S.C .Kuiry, "Ceria-Based High-Temperature Coatings for Oxidation Prevention", Jom-e, 52(1) , 2000, pp.163-177.
32. C. Houngninou, S. Chevalier and J.P. Larpin," Synthesis and Characterization of Pack Cemented Aluminide Coating on Metals", Applied Surface Science, Vol.236, Issues 1-4, 2004, pp.256-269.
33. D.F. Susan and A.R. Marder, "Oxidation of Ni-Al Base Electrodeposited Coatings; 1: Oxidation Kinetics and Morphology at 800C°", Oxidation of Metals, Vol.57, Nos.1/2, .2002, pp.131-157.

Table (1) Nominal composition and spectrochemical analysis of austenitic stainless steel (316L)

Element Wt%	C	Mn	Si	Cr	Ni	P	S	Mo	V	Cu	Fe
Nominal Value	<0.02	2.0	1.0	16-18	10-14	_	_	2-3	_	_	Rem
Measured Value	0.02	1.07	0.37	16.7	10.8	0.018	0.02	2.13	0.1	0.16	Rem

Table (2) The pack mixture composition and the heating cycle used in stainless steel (316L) pack cementation.

Power Pack Composition wt%							
Pack cementation process	Al	Si	Ce	NH4C1	$A1_2O_3$	Holding temperature C°	Coating Time (h)
Silicon modified aluminide diffusion coating process	18	7	-	2	73	970C°	2, 3, 4, 5 and 8h
Cerium doped silicon modified aluminide diffusion coating process	18	7	0.5	2	72.5	970C°	3h

Table (3): n values and linear oxidation rate constants k_L and parabolic oxidation rate constants Kp for cyclic oxidation of uncoated austenitic stainless steel 316L in air and H_2O vapor respectively for

Temperature C°	In Dry Air				In H_2O vapor
	n value	Kp ($mg^2/cm^4/s$	K_L (mg/ cm^2 /s)	n values	Kp ($mg^2/cm^4/s$)
700	0.5	$2.77*10^{-8}$		0.59	$0.755*10^{-5}$
800	1.0		$-2.77*10^{-7}$	0.52	$2.186*10^{-5}$
900	1.0		$-6.48*10^{-5}$	0.54	$2.675*10^{-5}$

100h at 10h cycle

Table (4): n values and parabolic oxidation rate constants K_P for cyclic oxidation of coated systems in air for 120h at 10 cycles.

Temperature C°	St.St.316L /A1Si		St.St.316L /AlSiCe	
	n values	Kp ($mg^2/cm^4/s$)	n values	Kp ($mg^2/cm^4/s$)
700	0.5	$1.6*10^{-6}$	0.5	$0.72*10^{-6}$
800	0.51	$2.77*10^{-6}$	0.6	$0.113*10^{-6}$
900	0.52	$3.15*10^{-5}$	0.38	$1.23*10^{-5}$

Table (5): n values and parabolic oxidation rate constants Kp for oxidation of coated systems in water vapor for 120h at l0h cycle.

Temperature C°	St.St.316L /A1Si		St.St.316L /AlSiCe	
	n values	Kp($mg^2/cm^4/s$)	n values	Kp($mg^2/cm^4/s$)
700	0.37	$0.447*10^{-5}$	0.5	$1.66*10^{-7}$
800	0.68	$1.725*10^{-5}$	0.72	$2.527*10^{-6}$
900	0.43	$2.166*10^{-5}$	0.77	$1.511*10^{-5}$

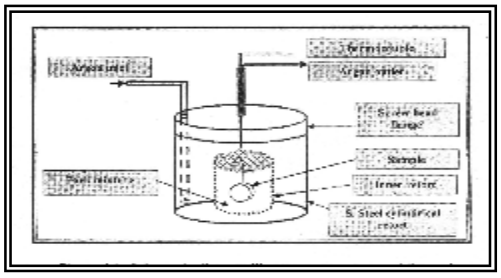

Figure(1) Schematic diagram illustrates apparatus used for pack cementation process.

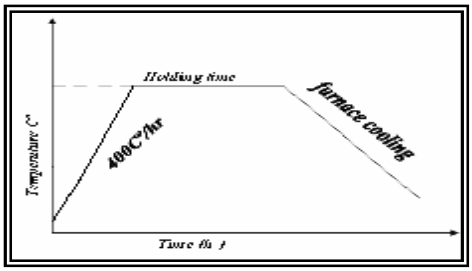

Figure (2) Heating cycle one step pack cementation process

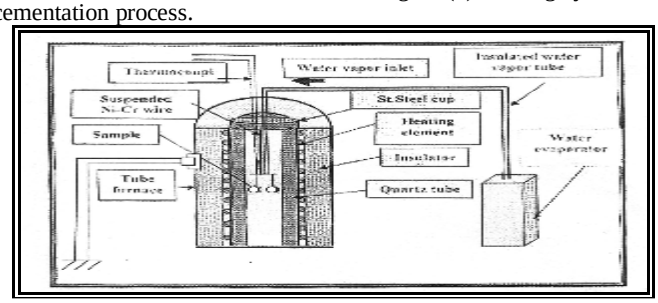

Figure (3) Schematic diagram illustrates apparatus used for high temperature cycle oxidation tests in water vapor (H_2O)

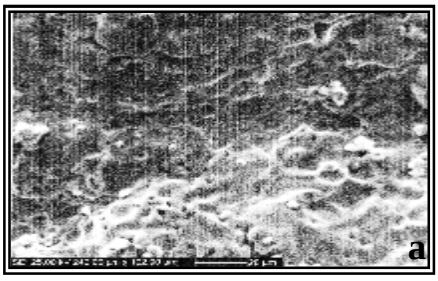

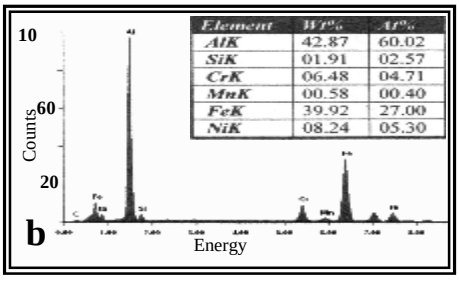

Figure(4): (a) SEM images of silicon-modified aluminide for St.St. 316L in the as coated . (b) EDX analyses showing the concentration variations of Al , Si and Fe near the surface at 970C° for 3h.

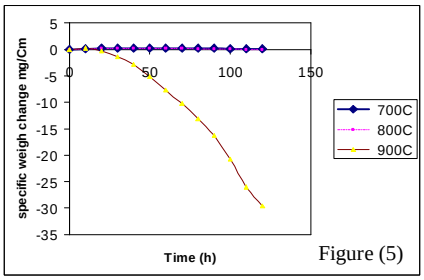

Figure (5)

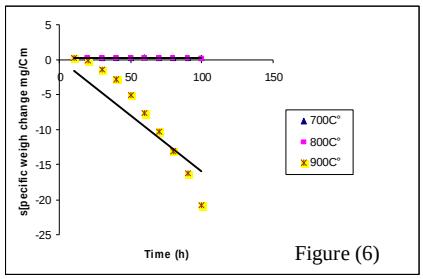

Figure (6)

Figure (5) Weight change vs- time plot for uncoated austenitic stainless steel 316L cyclic oxidized in air at temperatures between 700 and 900C° for 120 h at 10 h cycle.

Figure (6) Linear fitted results of weight change vs. time plot for uncoated austenitic stainless steel 316L cyclic oxidized in air at temperature between 700C° and 900C° for 120 h at l0h cycle .

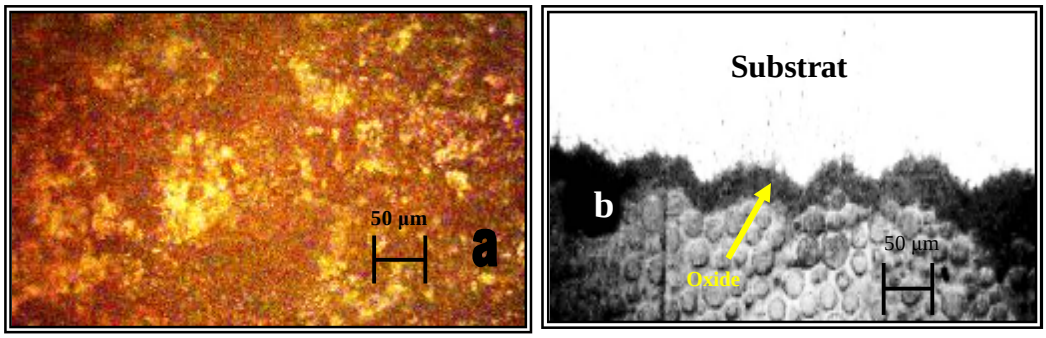

Figure (7): LOM images of surface scale growth uncoated stainless steel 316L after cyclic oxidation in air at 900C° for 120h at l0h cycle. (a) Top view (b) Cross section view

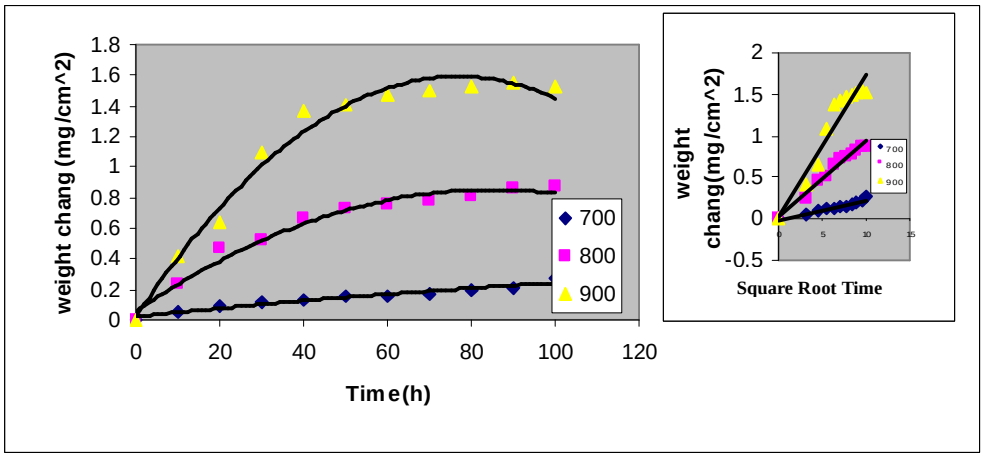

Figure (8) : Parabolic fitted results of weight change vs. time plot for uncoated austenitic stainless steel 316L cyclic oxidized in water vapor condition at temperatures between (700-900)C° for 120h at l0h cycle .

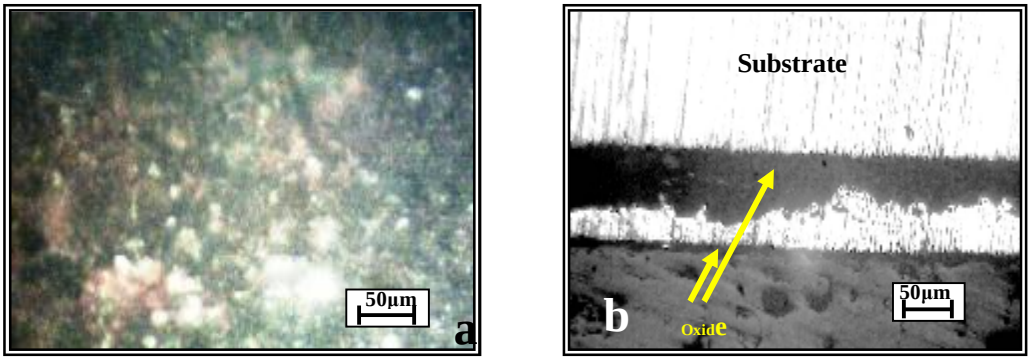

Figure (9): Low images of surface scale growth on uncoated stainless steel 316L after cyclic oxidation in water vapor condition at 900 C° for 120h at l0h cycle.
(a) Top view. (b) Cross section.

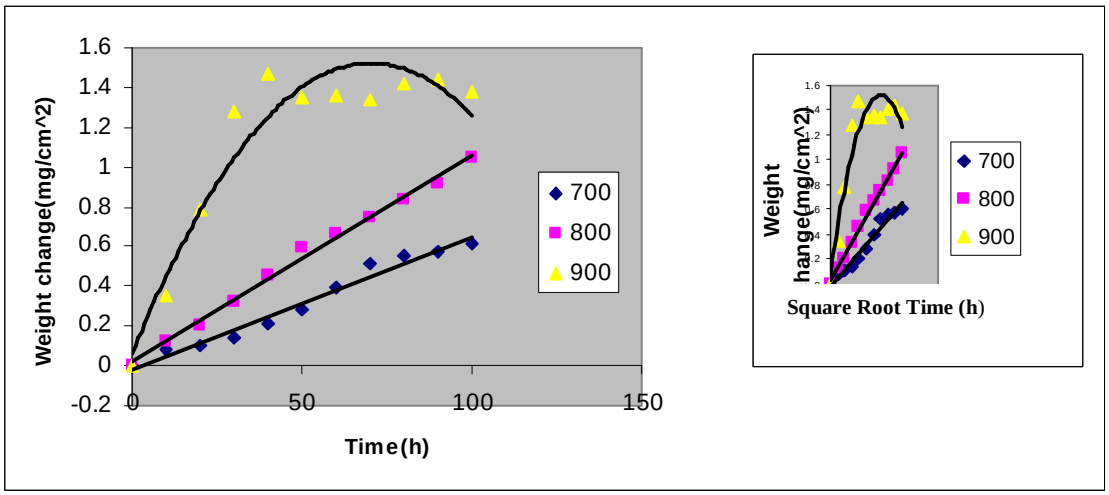

Figure (10): Parabolic and linear fitted results of weight change vs. time plot for silicon-modified aluminide diffusion coated austenitic stainless steel 316L substrates cyclic oxidized in air at temperatures between 700C°and 900C° for 120h at l0h cycle.

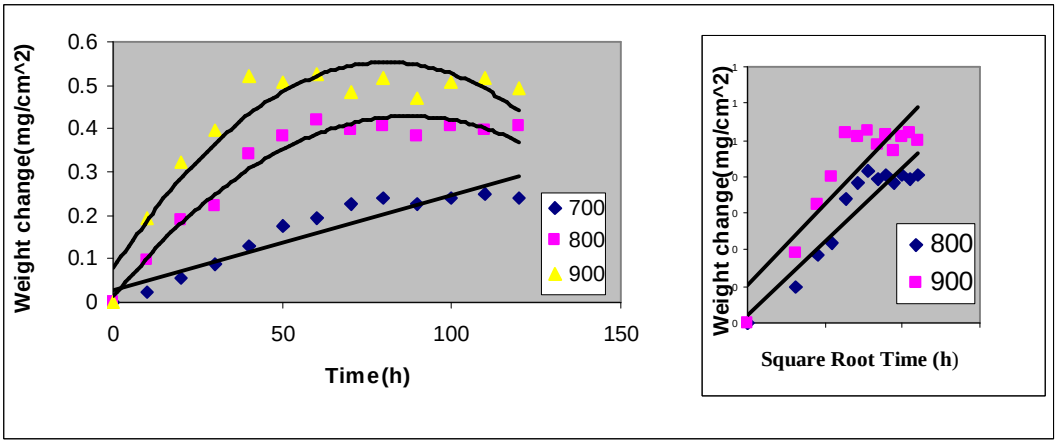

Figure. (11): Parabolic and linear fitted results of weight change Vs. time plot for cerium-doped silicon modified aluminide diffusion coated austenitic stainless steel 316L substrates cyclic oxidized in air at temperatures between 700C°and 900C° for 120h at l0h cycle.

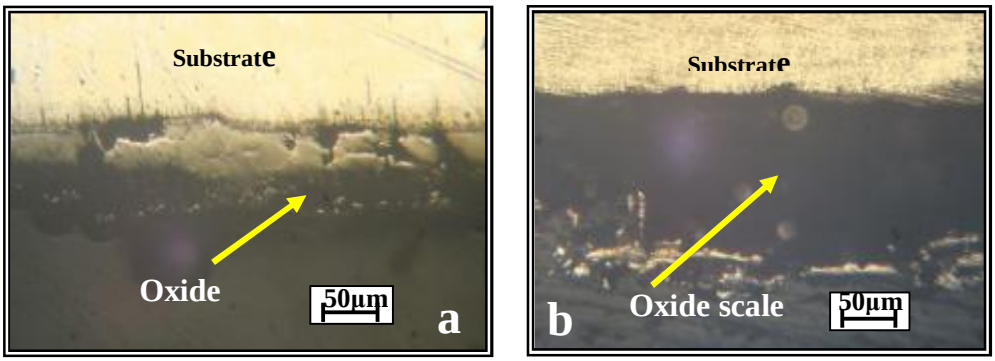

Figure(12): Cross section images of LOM of silicon-modified aluminide diffusion coated 316L substrates after cyclic oxidation in air at (a) 800C°, (b) 900C° for 120h at l0h cycle

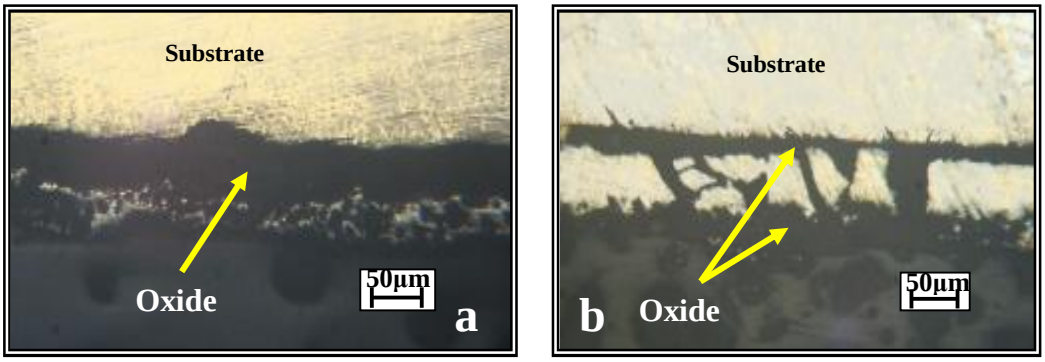

Figure (13): Cross section images of LOM of cerium-doped silicon-modified aluminide diffusion coated 316L substrates after cyclic oxidation in air at (a) 800C°, (b) 900C° for 120h at 10h cycle.

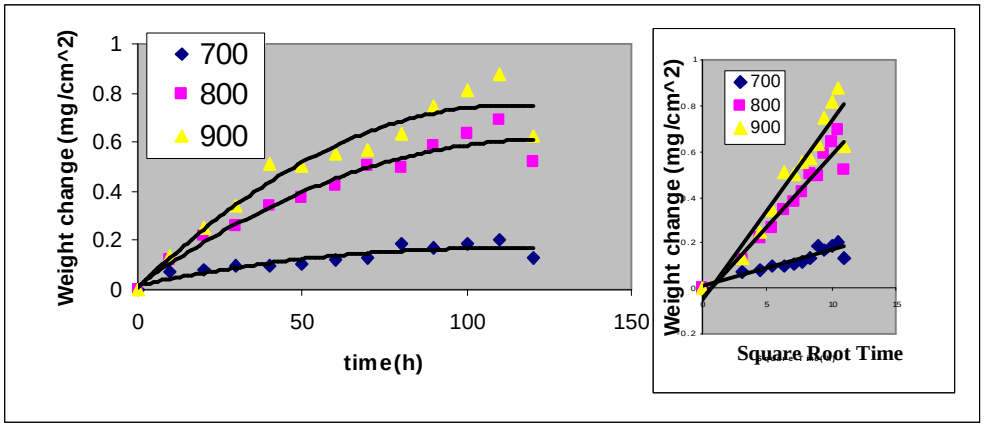

Figure(14): Parabolic fitted results of weight change Vs. time plot for silicon-modified aluminide diffusion coated 316L substrates cyclic oxidized under water vapor atmosphere between (700-900)C°, for 120h at 10h cycle.

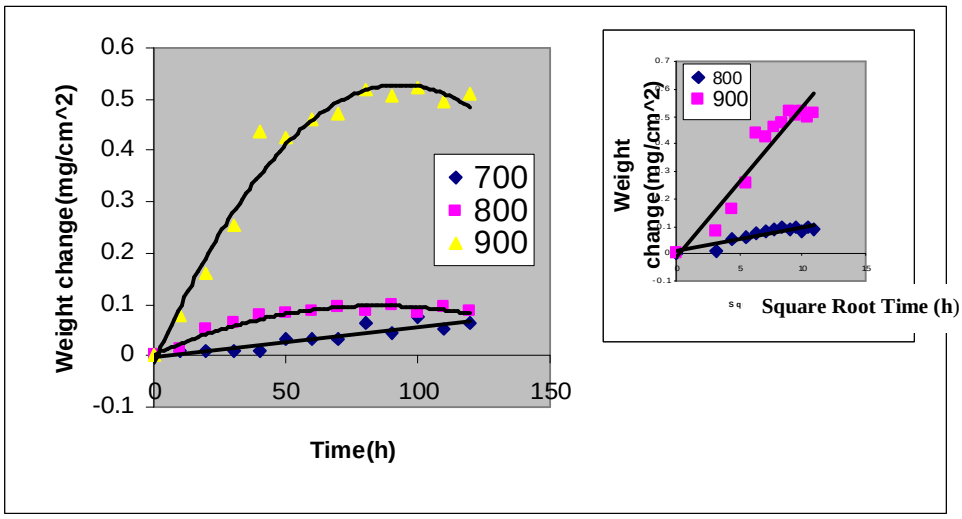

Figure(15): Parabolic fitted results of weight change Vs time plot for cerium doped silicon-modified aluminide diffusion coated 316L substrates cyclic oxidized under water vapor atmosphere between (700-900)C°, for 120h at l0h cycles

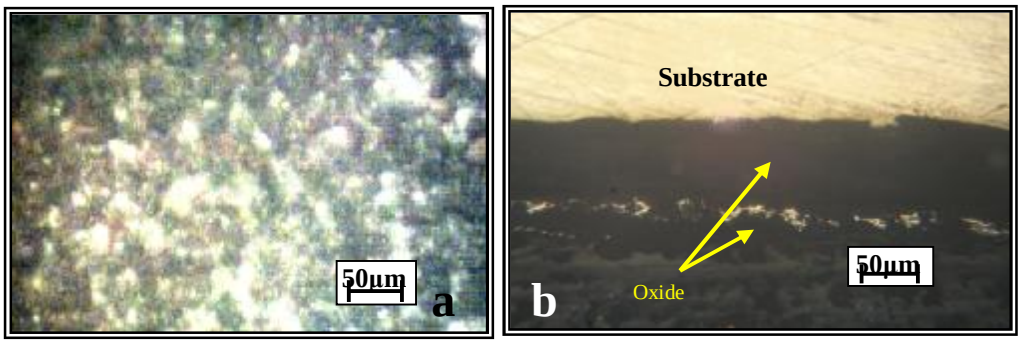

Figure (16): LOM images of cerium-doped silicon-modified aluminide diffusion coated stainless steel 316L substrates after cyclic oxidation under water vapor condition at 900C° for 120h at l0h cycle.(a) top view, (b) cross section view.

Appendixes

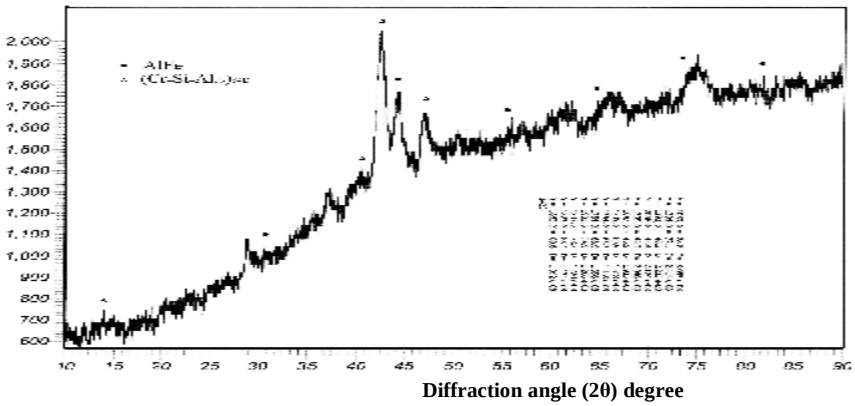

Fig.(A.1) Diffractograms from the surface of diffusion coated St.St.316L with silicon-modified aluminide for 3h coating time at 970C.

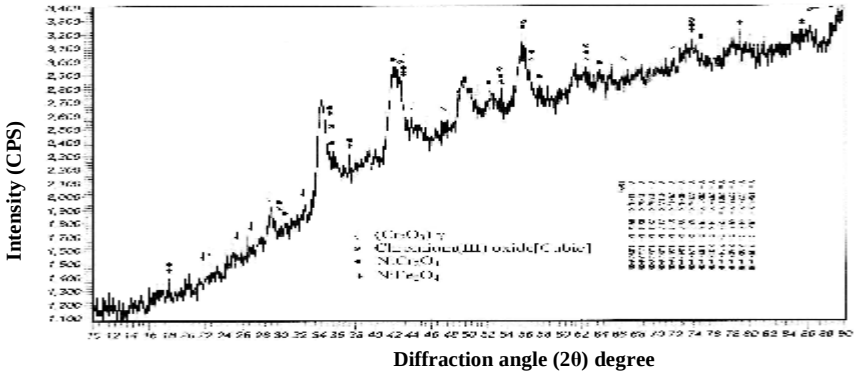

Fig.(A.2) Diffractograms from the surface of coated St.St.316L sample after cyclic oxidation in air at 900C°, for 120h at 10h cycle.

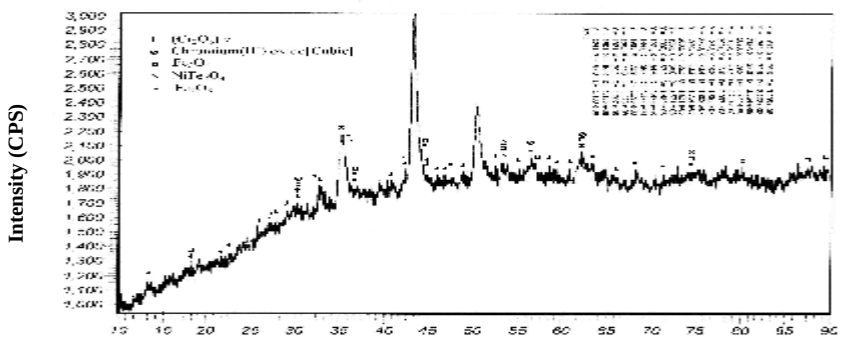

Fig.(A.3) Diffractograms from the surface of coated St.St.316L sample after cyclic oxidation under water vapor condition at 900C°, for 120h at 10h cycle.

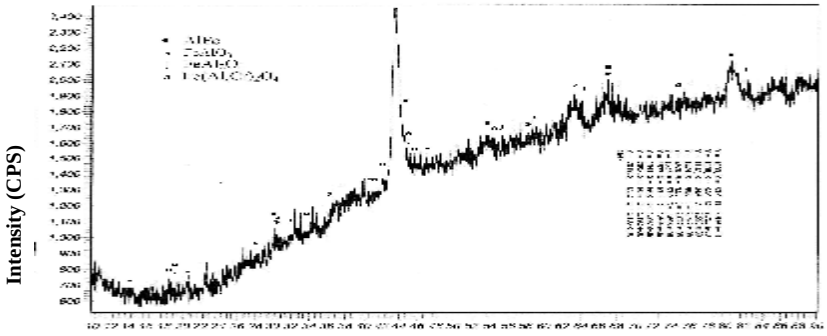

Fig.(B.1) Diffractograms from the surface of coated St.St.316L with silicon-modified aluminide diffusion coated sample after cyclic oxidation in air at 900C°,for 120h at 10h cycle.

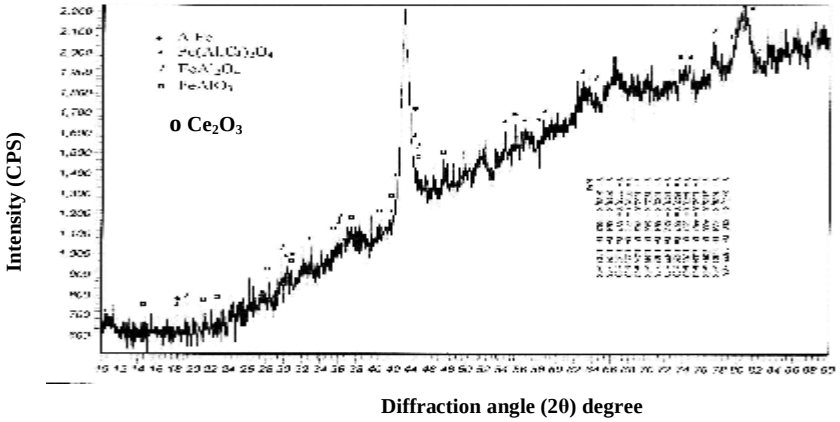

Fig(C.1) Diffractograms from the surface of coated St.St.316L with cerium-doped silicon-modified aluminide diffusion coated sample after cyclic oxidation in air at 900C°, for 120h at 10h cycle.

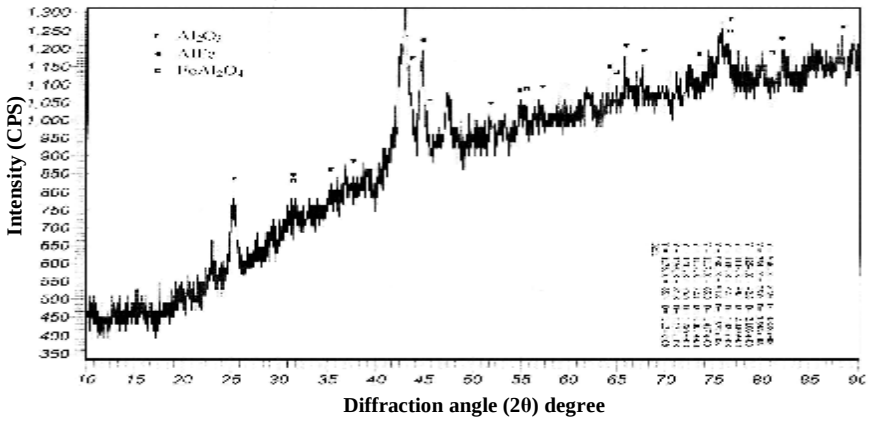

Fig (B.2) Diffractograms from the surface of coated St.St.316L with silicon-modified aluminide diffusion coated sample after cyclic oxidation under water vapor at 900C°,for 120h at 10h cycle.

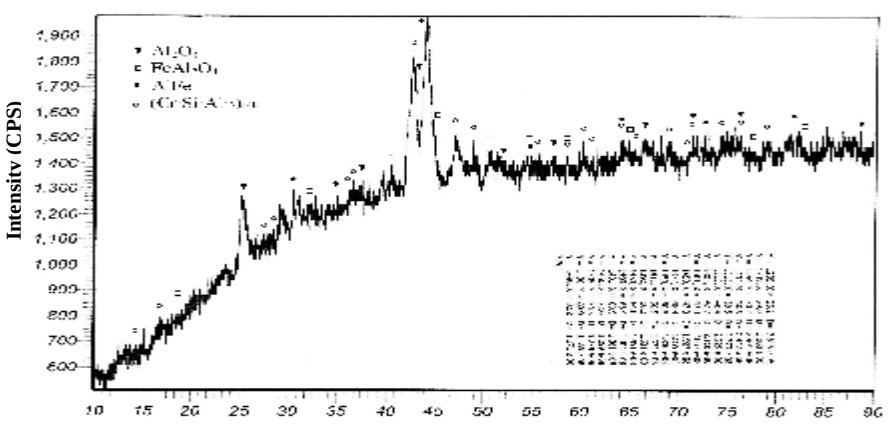

Fig (C.2) Diffractograms from the surface of coated St.St.316L with cerium-doped silicon-modified aluminide diffusion coated sample after cyclic oxidation in water vapor at 900C°, for 120h at 10h cycle.